doi:10.14311/ppt.2025.2.136
Plasma Physics and Technology **12**(2):136–141, 2025

FREE BURNING ARC BLACK-BOX MODELING IN CO_2/O_2

T. Gfrörer*, C. M. Franck

High Voltage Laboratory, ETH Zurich, Physikstrasse 3, 8092 Zurich, Switzerland

* gfroerer@eeh.ee.ethz.ch

Abstract. Black-box arc parameters were fitted from free-burning arc experiments in a 3 bar abs. CO_2/O_2 (90%/10%) mixture for the first time. Best fits were achieved with a novel Cassie-based model for low-current arcs. Averaged arc time parameters were $\tau \approx 170\,\mu s$ at low currents (20–50 A) and $\tau \approx 33\,\mu s$ at high currents (1–3 kA), respectively. A decrease of τ could be observed for elongated arcs. Explanations based on thermodynamic arc properties are consistent with measured variations of τ.

Keywords: black-box arc models, SF_6-alternatives, switching arcs, arc discharge, CO_2/O_2-mixtures.

1. Introduction

SF_6 is widely used in high-voltage equipment as an insulation and arc-quenching medium, but has a high global warming potential and needs to be replaced by more climate-friendly alternatives [1]. CO_2-based gases were first used in high voltage circuit breakers (HVCB) by Uchii et al. [2] to replace SF_6.

Black-box modeling is used in HVCB short-line fault (SLF) testing to predict limiting values for $\mathrm{d}i/\mathrm{d}t$ and to describe the influence of external circuitry on limiting $\mathrm{d}i/\mathrm{d}t$ [3]. Some papers have experimentally determined and published parameters for black-box models in CO_2, and specified arc time parameters varying from 0.3–3.3 µs under various blown [4–8], and from 13–76 µs in unblown cage-stabilized conditions at 3 bar abs. and between 1–6 A [9]. However, no experiment has provided both parameter validation—the comparison between predicted and measured arc voltage—and specified all factors influencing arc parameters, including blow pressure. More experiments should be performed specifying all relevant conditions and proving the validity of fitted arc parameters.

This paper investigates black-box arc parameters in a CO_2/O_2 mixture in a free-burning arc experiment as in Pietrzak et al. [10], with conditions similar to disconnector switching operations. These experiments serve as a preparation for experiments under blown-arc conditions. A flexible pulsed current source (FPCS) [11] was used to perform the experiments, enabling the extraction of more than 800 arc parameter estimates independently with only few arcing experiments. The method for parameter extraction was adapted from Walter and Franck [12]. Black-box models used were based on the Cassie [13] and Mayr [14] models, and the Mayr-Schwarz [15] model with a power function for cooling power. Some models were extended with a separate electrode enhancement voltage [16, 17] as in Christen and Ranjan [18]. Fitted arc time parameters are discussed with arc temperature measurements [17, 19, 20] and thermodynamic gas properties [21–23].

2. Methods

2.1. Experiment

To be able to observe transient arc behavior, the change of arc current has to be large enough for the arc voltage to deviate from the steady-state voltage. Arc voltage response is shown for different di/dt in Figure 1. To generate such rapidly changing currents, the FPCS is used, consisting of 1 to 8 modules of parallel-connected buck-type converters, shown in Figure 2. Experiments in CO_2/O_2 (90%/10%) are performed in the free-burning arc setup, shown in Figure 3. In Table 1, details on additional measurement instruments are given. The chronology of current through the arc and opening of the pins is described in Figure 4.

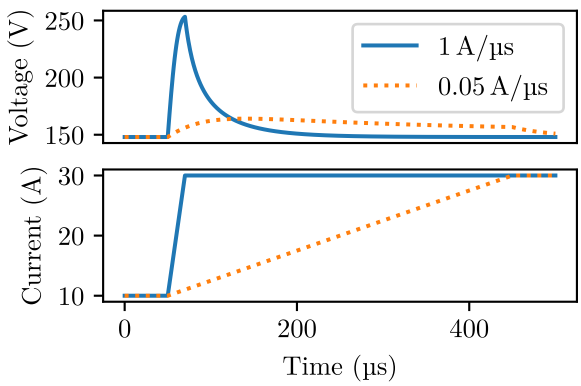

Figure 1. Dynamic voltage response simulated with the ElCassie model from Table 2 ($U_C = 100\,\mathrm{V}$, $\tau = 100\,\mu s$). The 1 A/µs pulse yields a transient voltage response significantly higher than the steady-state arc voltage.

2.2. Black-box Models

We use models based on the Mayr-Schwarz arc model [15], but with a constant arc time parameter τ, see (1). i is measured current, g model predicted conductance.

$$\frac{\mathrm{d}g}{\mathrm{d}t} = \frac{1}{\tau}\left(\frac{i^2}{P(g)} - g\right) \tag{1}$$

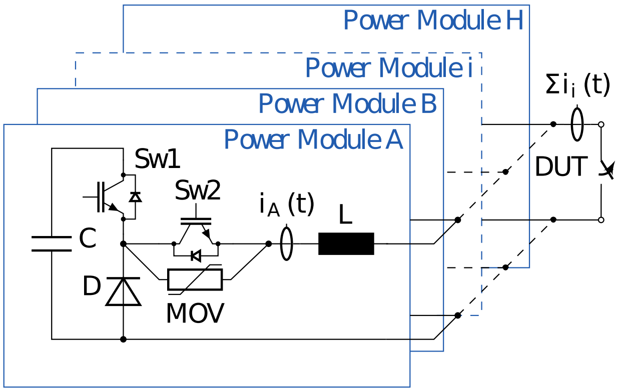

Figure 2. Adapted from [11]: The FPCS can increase the current through the device under test (DUT) rapidly by closing Sw1 and Sw2. Current freewheels through the diode when Sw1 is open, yielding a slowly decaying current at low load voltages. Output current hysteresis control is applied.

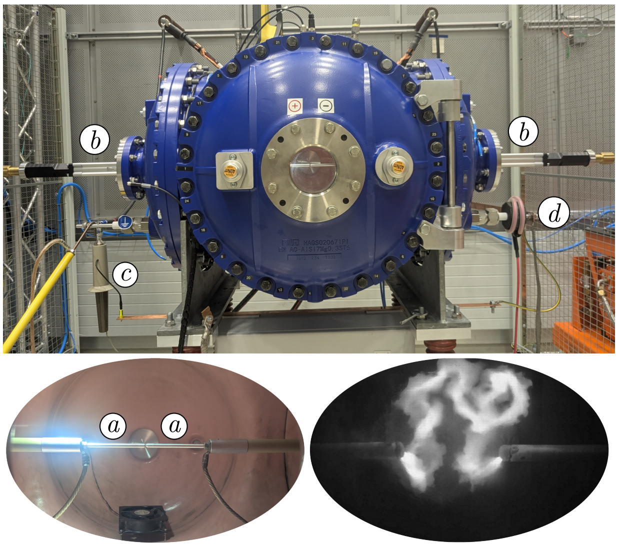

Figure 3. Free-burning arc experiments are performed by first initiating a current, followed by an opening of the arcing contacts (a) initiated by pneumatic cylinders (b). Arc voltage is measured by a 1:1000 Tektronix P6015A voltage probe (c), current by a PEM CWT30 Rogowski coil (d). All experiments are recorded with a high-speed camera (not shown here).

The cooling power $P(g)$ defines the steady state behavior of the arc. We use $P(g) = A \cdot g^b$, where A is freely chosen during fitting. b is either a fixed or a free parameter. Together, A, b and τ make up the arc parameters.

We extend some arc models by an electrode enhancement voltage u_{el}, measured by Engelbrecht et al. [17] in the same experimental setup as here and under similar conditions. This yields the predicted voltage u_{pred} from (2).

$$u_{\mathrm{pred}} = u_{\mathrm{el}} + i/g \tag{2}$$

Having a separate model for the electrode enhancement voltage is beneficial since in our experiment, it makes up a significant portion of the total arc voltage, and the physical processes describing it are different than in the rest of the arc, as described in [17].

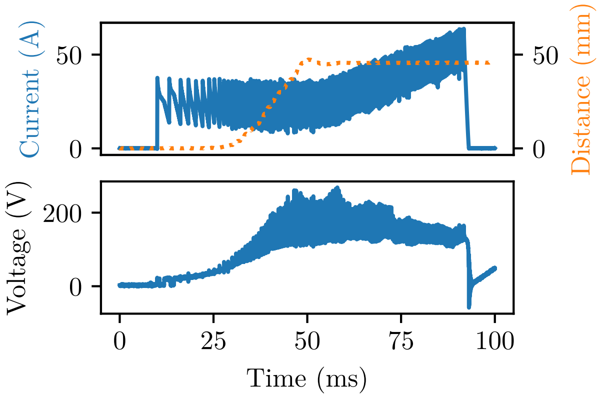

Figure 4. Arc #290: First, the FPCS initiates a low current (10 ms) while the pins are still closed. Then, pins are opened and an arc forms. As soon as the pins are fully opened (50 ms), the current is varied to probe arc parameters at different current levels. A single current peak is shown in Fig. 5.

Type	**Sensor**	**Range**
Pressure	Wika S-20	2.99 to 3.01 bar
Temperature	Wika TF-35	20 to 22 °C
Humidity	Wika GDHT-20	−38 to −33 °C
Distance	Festo 1531266	44.0 to 47.7 mm

Table 1. Measurements of temperature and pressure performed just before ($\ll 1$ s) current initiation. Humidity (dew point) measurements were performed at 5 bar abs. before the experiments, and at 1 bar abs., after the experiments at 3 bar abs. Pin separation is given for values 40 ms after current initiation.

The different model settings used are shown in Table 2. All model names for models with $u_{\mathrm{el}} = 48$ V are prefixed with an 'El'. The models with b as a free parameter are called Power models. The model with b fixed to 1.35 is called ElPowerFixed. The Cassie and ElCassie models are equivalent to the Power / ElPower model with $b = 1$ and predict a constant steady-state arc voltage. For the Cassie and ElCassie models, the Cassie voltage $U_{\mathrm{C}} = \sqrt{A}$ can be defined. Derived from this, $U_{\mathrm{C}} + u_{\mathrm{el}}$ is the stationary / steady-state arc voltage. For other models with $b \neq 1$, U_{C} is undefined, and no steady-state voltage exists, since the steady-state voltage would vary with current. The Mayr and ElMayr models are equivalent to the Power / ElPower model with $b = 0$ and predict a constant cooling power $P(g) \equiv A$.

2.3. Data Evaluation

Voltage u_{meas} and current i time-series data are acquired with a Lecroy HDO6054 oscilloscope at 100 MS/s and 20 MHz bandwidth-limit, lowpass-filtered with a pass-band frequency of 1 MHz and

Name	b	$u_{\mathbf{el}}(V)$
ElCassie	1	48
ElPowerFixed	1.35	48
Cassie	1	0
ElMayr	0	48
Mayr	0	0
ElPower	free	48
Power	free	0

Table 2. The ElCassie model is used for all low-current fits. The ElPowerFixed model is used only for the high-current arc fits. All the other models are used for fits with one low-current arc #290 to compare fit quality.

then downsampled. To describe only the arc voltage, and not the inductive or resistive voltage drop of the wiring, both voltage drops are compensated by subtracting them from the measurement. Compensating the inductive voltage drop introduces a lot of noise, as it requires the calculation of the time-derivative of measured current, and is therefore only possible with previously performed low-pass filtering. Since the current is measured with a CWT30 Rogowski coil, the droop of the current probe has to be compensated for.

Parameter fits are performed over a time defined as the fitting window length t_{window}, visible in an example of a fit shown in Fig. 5. Current rise begins at $t = 0.3 \cdot t_{\text{window}}$. Only current peaks with $t > 50\,\text{ms}$ are used when the pins are fully opened; see Fig. 4.

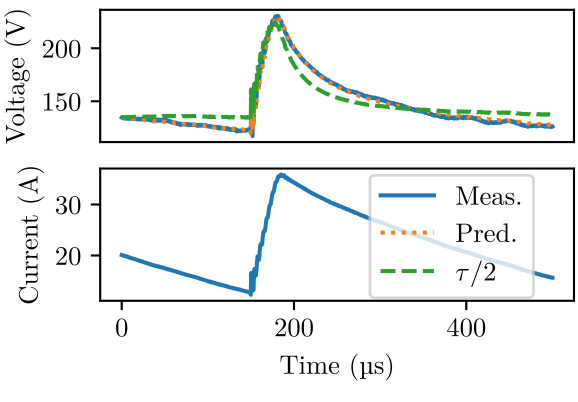

Figure 5. First fit of arc #290 with the ElCassie model, with fitting loss $= 2.0\,\mathrm{V}_{RMS}$, $U_C = 105\,\mathrm{V}$, $\tau = 202\,\mu\mathrm{s}$ and $g \in [0.10\,\mathrm{S}, 0.18\,\mathrm{S}]$. The arc voltage increases after rapid rise of current, as conductance takes a long time τ to increase, and decrease the voltage to the steady-state voltage $U_C + u_{el}$. Voltage then undershoots this steady-state voltage due to decreasing current. The predicted voltage with halved $\tau = 101\,\mu\mathrm{s}$ but same U_C is shown to prove that a significantly larger τ than $101\,\mu\mathrm{s}$ is required to adequately describe the arc voltage.

For each current peak individually, the arc parameters are first initialized to values that are reasonably close to the optimal parameters. This makes it more likely that the global optimum of parameter estimates can be found. Usually, the parameters are initialized to the last parameter fit, but they can also be initialized from other parameter fits, or from a simplified calculation of the parameters A and b, and trying out different τ. The initial conductance at the start of the fitting window is calculated as $g_0 = i_0/(u_0 - u_{\text{el}})$ from the initial measured current i_0 and voltage u_0. The parameters are estimated with nlgreyest from the MATLAB System Identification Toolbox with the Levenberg–Marquardt algorithm. The algorithm chooses parameters to minimize the cost function (3).

$$C = \frac{1}{t_{\text{window}}} \int_0^{t_{\text{window}}} (u_{\text{pred}}(t) - u_{\text{meas}}(t))^2 \text{d}t \quad (3)$$

From u_{pred} and u_{meas}, the fit percentage can be calculated. If it is above 0, and nlgreyest terminated with solution "near a (local) minimum", fit parameters are accepted. Otherwise, the parameter estimation is repeated with a different parameter initialization, if available.

For low current arcs, $t_{\text{window}} = 500\,\mu\text{s}$ was used. t_{window} should be significantly larger than τ, since it was observed that estimated τ are biased towards lower values otherwise. For $t_{\text{window}} = 500\,\mu\text{s}$, τ was insensitive to small changes in t_{window}. For the high-current arcs, it was adequate to reduce t_{window} to $180\,\mu\text{s}$.

Arc instabilities cannot be predicted by black-box models. If they occur rapidly as in Fig. 10, this yields a high loss $:= \sqrt{C}$. Low-current (20–50 A) peaks are included with loss $\leq 4\,\text{V}_{\text{RMS}}$ (838/843 included from arcs #290–297), and high-current (1–3 kA) peaks with loss $\leq 10\,\text{V}_{\text{RMS}}$ (30/31 included from arc #289). Experimental results in the range of 50–1000 A are not shown, due to reasons discussed in section 4.3.

Arc parameters are plotted against middle current $i_{\text{mid}} := (i_{\text{min}} + i_{\text{max}})/2$ to show the dependency of arc parameters on arc current. $\forall t_{\text{window}} : i_{\text{min}} := \min_{t_{\text{window}}} i$ and $i_{\text{max}} := \max_{t_{\text{window}}} i$.

3. Results

The results of the experiments performed at the lowest currents are shown in Figure 6. Only one experiment was performed at the highest current level due to excessive pin contact ablation. The result is shown in Fig. 7. The results of the low-current experiments show negative linear correlations between U_{C} and τ, as well as between i_{mid} and U_{C}, but not between i_{mid} and τ, see Tab. 3. To give an idea of how good the fits are, see Fig. 5, where the current and voltage measurement, and the predicted voltage, are shown.

4. Discussions

Averaged τ at high currents (1–3 kA) in CO_2/O_2 are a factor of 5 lower than at low currents (20–50 A).

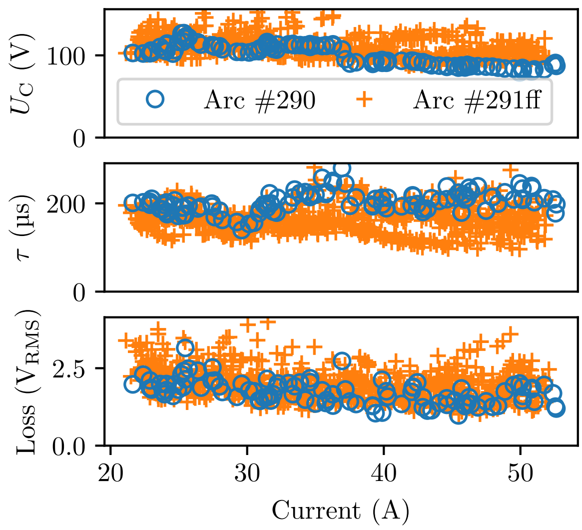

Figure 6. Arc parameters and fitting loss of low-current arcs plotted against middle current i_{mid}. Averaged values are $\bar{U}_C = 108\,\mathrm{V}$, $\bar{\tau} = 170\,\mathrm{\mu s}$, $\overline{Loss} = 2.0\,\mathrm{V}_{RMS}$ and $\overline{FitPercent} = 88\%$.

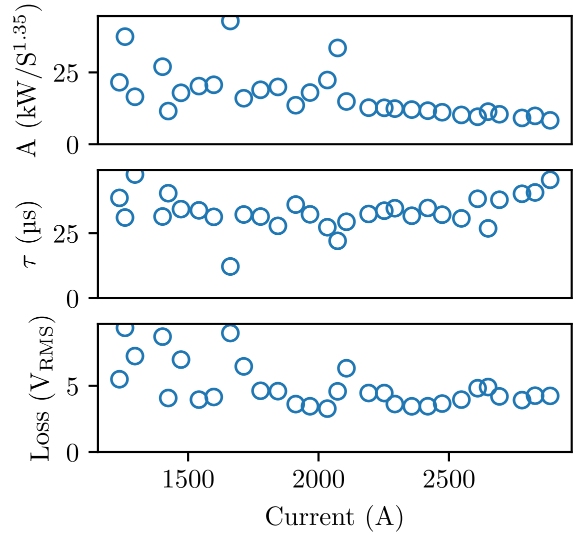

Figure 7. Parameter fits for highest-current experiments. Below 2.1 kA, strong arc instability occurred, visible in large fluctuations in parameter A. τ is much shorter than for the low-current experiments, with an average of $\bar{\tau} = 33\,\mathrm{\mu s}$, $\overline{Loss} = 5.0\,\mathrm{V}_{RMS}$ and $\overline{FitPercent} = 71\%$.

Within these current regimes, τ does not correlate significantly with current; see Tab. 3. However, a negative correlation between τ and U_C can be observed for the low-current arcs. Wherever τ for arc #290 is higher in Fig. 6 than for arcs #291ff, U_C is lower. The reason for the observed negative correlation is unknown. An increased U_C at the same current directly corresponds to an increased steady-state arc voltage, which in turn is caused in free-burning arcs most likely through arc excursions, i.e. arc elongation. This phenomenon can be directly observed in Fig. 10

(i,j)	$r_{i,j}$	$p_{i,j}$	Slope
(i_{mid}, U_C)	-0.45	$< 10^{-42}$	$-0.63\,\mathrm{V/A}$
(i_{mid}, τ)	0.03	0.39	N/A
(U_C, τ)	-0.50	$< 10^{-53}$	$-1.26\,\mathrm{\mu s/V}$

Table 3. Pearson correlation coefficient $r_{i,j}$, p-value $p_{i,j}$ and slope of linear regression calculated for the low current arc parameter fits.

in a more violent arc voltage collapse.

4.1. Physical Interpretation

4.1.1. Higher Arc Time Parameter at Low Currents

One factor influencing τ is the product of specific heat and density of the arc ρC_p. Other factors like thermal conduction, convection and radiative losses could additionally affect τ, but were not investigated in this contribution. Assuming a positive correlation, i.e. a higher ρC_p yields a higher τ, it could be hypothesized that an increase of ρC_p at lower currents compared to higher current could be responsible for the increase of τ at low currents. In an experiment under conditions similar to those in this paper ($CO_2/O_2/C_5F_{10}O$ with 85%/10%/5%, 45 mm contact gap, 1 bar abs. pressure), the arc temperature was measured to be 10 kK at $i > 1\,\mathrm{kA}$ ($N = 8$, $\sigma_T = 700\,\mathrm{K}$), while for the final measurement the arc temperature was 8.6 kK at 420 A [17]. Assuming a similar temperature decrease from high to low currents in our experiment, this would yield significantly increased ρC_p, as pure CO_2 has a local ρC_p maximum at 7.2 kK [21], 7.9 kK [22] or 8.0 kK [23], and no significant difference to CO_2/O_2 (90%/10%) is present [23]. ρC_p is much lower at 10 kK compared to the local maximum mentioned above; see Fig. 8.

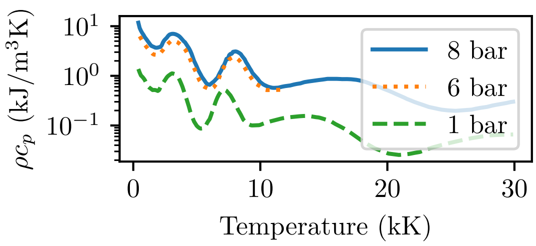

Figure 8. ρc_p of CO_2 at 1 bar [21], 6 bar [22] and 8 bar abs. [23]. The local maximum between 7.2–8 kK may be responsible for increased τ at low currents.

4.1.2. Comparison to Cage-Stabilized Experiments

Arc parameters fitted by Yoon and Spindle [9] are the most fair comparison to arc parameters presented here. While we measured τ down to 20 A with $\bar{\tau} = 170\,\mathrm{\mu s}$, Yoon and Spindle [9] measured only up to 6 A. Assuming that at 6 A, the arc temperature has decreased below the local ρC_p maximum mentioned in subsection 4.1.1, their measurements of 13–21 µs at 1 A and 76 µs at 6 A may still be compatible with our measurements. This assumption is supported by arc temperature measurements, placing the arc temperature of a free-burning CO_2 arc at ambient pressure to 6500–7200 K between 0.4–1.3 A of current according to Becerra et al. [19], or to 5500 K at 3.5 A according to Billoux et al. [20].

4.2. Model Choice

Experiments were fitted not just with one model, but with many, to find the best model. A box plot of τ and loss function for the fits of low-current arc #290 / high-current arc #288 is shown in Figure 9. The ElCassie model is adequate for stable low-current arcs in CO_2/O_2. The additional fitting parameter in ElPower is unnecessary and may in fact lead to overfitting, as seen by the standard deviation of estimated b being $\sigma_b = 0.31$. All other models tested perform worse than the ElCassie model, indicating that separate modeling of u_{el} is necessary for arcs with a significant voltage contribution by the electrodes. The constant $\mathrm{d}u/\mathrm{d}i$ observed in our experiments at low currents, and the more accurate separate model of the electrode enhancement voltage make the ElCassie model the best choice for modeling low-current, free-burning arcs in CO_2/O_2. τ is heavily dependent on the choice of u_{el}, and somewhat dependent on the choice of b, if this choice is suboptimal.

High-current experiments required a choice of $b > 1$, since they showed $\mathrm{d}u/\mathrm{d}i > 0$. Optimal fits were achieved with $b = 1.35$, which was chosen as the median b estimated with the ElPower model. The loss of the ElPowerFixed model is clearly lower than the loss of the ElCassie model, see Figure 9.

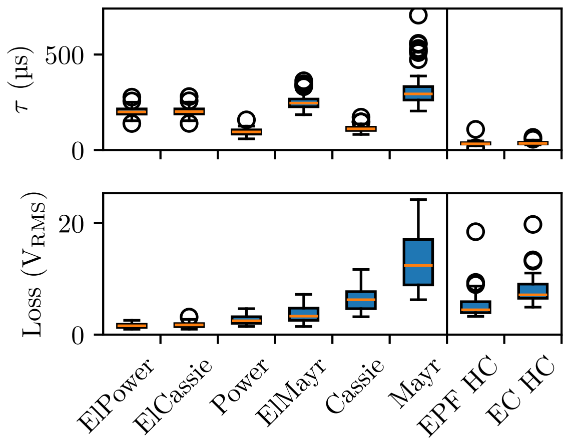

Figure 9. Box plot showing τ and fitting loss of low-current arc #290 / high-current arc #288 using different models. Best fits are made for low currents with ElPower and ElCassie models, yielding consistent estimates of τ. All other models, including the power model with three free parameters, perform worse. For high currents, fits made with the ElPowerFixed model (labeled EPF HC) outperform ElCassie model (EC HC) fits, but estimates of τ are similar for both models.

4.3. Arc Instability

Experiments in CO_2/O_2 at 3 bar abs. were shown for 20–50 A and 1–3 kA only. Experiments with currents in between showed much larger arc instability. Arc instability results in either a gradual change of arc length (and therefore arc voltage) or a rapid collapse of arc voltage, shown in Fig. 10. Whereas arc voltage collapse yields time-series data that cannot be fitted solely with black-box models, it is unclear whether slow arc instabilities could bias arc parameter estimation, wherefore only experiments with fairly stable arcs were shown. Two experiments at 20–50 A were also unstable, and were not included in the analysis.

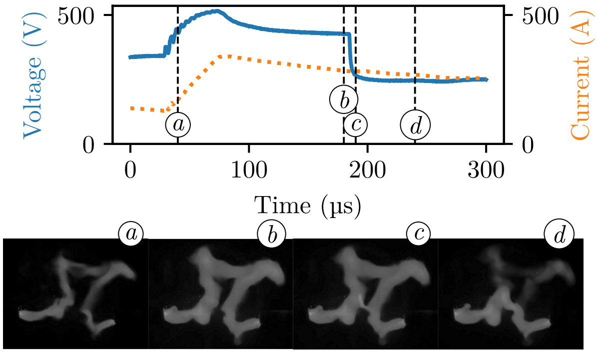

Figure 10. Experiment performed in SF_6 at 3 bar. At the start of the current increase (a), the arc is elongated. Over time it becomes brighter and expands (b). This leads to breakdown between sections of the arc (c), leading to voltage collapse. The shorted part of the arc cools and becomes less bright (d).

5. Conclusions

We performed free-burning arc experiments in a 3 bar abs. CO_2/O_2 (90%/10%) mixture at low (20–50 A) and high (1–3 kA) currents. The FPCS was used to generate many current peaks in short succession, enabling the extraction of > 800 independently fitted arc parameters. A novel 2-parameter black-box model, based on the Cassie model but extended with a separate electrode enhancement voltage u_{el} was able to best predict the arc voltage from the arc current at 20–50 A. Using 3-parameter black-box models did not improve the predicted voltage accuracy. Mayr, Cassie and Power models performed significantly worse than the novel ElCassie model.

Averaged arc time parameter τ was a factor of 5 higher at 20–50 A compared to 1–3 kA. An explanation based on the product of specific heat and density ρC_P was suggested. A negative correlation between Cassie voltage U_{C} and τ was observed in low current arcs. The cause of this is yet unknown.

Future research will also evaluate arc parameters for arcs with more instabilities, at different pressures and in different gas mixtures, as well as under blown conditions. Furthermore, a calculation method for calculating the uncertainty of the estimated parameters must be established.

Acknowledgements

We thank Hitachi Energy for financially supporting this project and Martin Seeger from Hitachi Energy for all the critical discussions.

References

[1] CIGRÉ WG A3.41. "Current Interruption in SF6-free Switchgear". CIGRÉ Technical Brochure no. 871, 2022.

[2] T. Uchii, Y. Hoshina, T. Mori, et al. "Investigations on SF6-Free Gas Circuit Breaker Adopting CO2 Gas as an Alternative Arc-Quenching and Insulating Medium". In L. G. Christophorou, J. K. Olthoff, and P. Vassiliou, editors, *Gaseous Dielectrics X*, pages 205–210. Springer US, Boston, MA, USA, 2004. ISBN 978-1-4419-8979-6. doi:10.1007/978-1-4419-8979-6_28.

[3] CIGRÉ WG 13.01. "State of the art of circuit-breaker modelling". CIGRÉ Technical Brochure no. 135, 1998.

[4] K. Mochizuki, T. Ueno, H. Mizoguchi, et al. "Evaluation of Interruption Capability on Various Gases". In L. G. Christophorou, J. K. Olthoff, and P. Vassiliou, editors, *Gaseous Dielectrics X*, pages 265–270. Springer US, Boston, MA, USA, 2004. ISBN 978-1-4419-8979-6. doi:10.1007/978-1-4419-8979-6_37.

[5] T. Matsumura, I. Morooka, Y. Yokomizu, and M. Suzuki. "Arc Parameters in CO2-blast quenching chamber with high-pressure storage tank of different pressures". *Vacuum*, 80(11-12):1305–1310, Sept. 2006. doi:10.1016/j.vacuum.2006.01.034.

[6] S. Nishiwaki, T. Koshizuka, T. Uchii, and H. Kawano. "Discussions on Post Arc Current of a CO2 Circuit Breaker". In *2008 17th Int. Conf. Gas Discharges Their Appl.*, pages 125–128, 2008. ISBN 978-0-9558052-0-2.

[7] K. Udagawa, T. Koshizuka, T. Uchii, et al. "CO2 Circuit Breaker Arc Model for EMTP Simulation of SLF Interrupting Performance". In *Int. Conf. Power Syst. Transients (IPST2011)*, Delft, Netherlands, 2011. 11IPST037.

[8] Z. Guo, S. Liu, Y. Pu, et al. "Study of the Arc Interruption Performance of CO2 Gas in High-Voltage Circuit Breaker". *IEEE Trans. Plasma Sci.*, 47(5):2742–2751, May 2019. doi:10.1109/TPS.2019.2904981.

[9] K. H. Yoon and H. E. Spindle. "A Study of the Dynamic Response of Arcs in Various Gases". *Trans. Amer. Inst. Elect. Engineers. Part III: Power App. Syst.*, 77(3):1634–1640, Apr. 1958. doi:10.1109/AIEEPAS.1958.4500218.

[10] P. Pietrzak, J. T. Engelbrecht, P. Simka, et al. "Voltage-Current Characteristic of Free Burning Arcs in SF6 Alternative Gas Mixtures". *IEEE Trans. Plasma Sci.*, 50(11):4744–4752, Nov. 2022. doi:10.1109/TPS.2022.3210995.

[11] H. Janssen, P. Devaud, T. Wei, and C. M. Franck. "A flexible pulsed current source to characterise future switching technologies". In *23rd Int. Symp. High Voltage Eng. (ISH 2023)*, volume 2023, pages 554–560, 2023. doi:10.1049/icp.2024.0579.

[12] M. Walter and C. Franck. "Improved Method for Direct Black-Box Arc Parameter Determination and Model Validation". *IEEE Trans. Power Del.*, 29(2):580–588, Apr. 2014. doi:10.1109/TPWRD.2013.2283278.

[13] A. M. Cassie. "Arc Rupture and Circuit Severity: A New Theory". In *Conf. Int. Grands Réseaux Életriques Haute Tension*, Paris, FR, Jun./Jul. 1939.

[14] O. Mayr. "Beiträge zur Theorie des statischen und des dynamischen Lichtbogens". *ETZ-A*, 37(12):588–608, Dec. 1943. doi:10.1007/BF02084317.

[15] J. Schwarz. "Dynamisches Verhalten eines gasbeblasenen, turbulenzbestimmten Schaltlichtbogens". *ETZ-A*, 92(3):389–391, 1971.

[16] Y. Yokomizu, T. Matsumura, R. Henmi, and Y. Kito. "Total voltage drops in electrode fall regions of SF6, argon and air arcs in current range from 10 to 20 000 A". *J. Phys. D: Appl. Phys.*, 29(5):1260–1267, May 1996. doi:10.1088/0022-3727/29/5/020.

[17] J. T. Engelbrecht, P. Pietrzak, and C. M. Franck. "Cu/W Electrode Ablation and Its Influence on Free-Burning Arcs in SF6 Alternatives". *IEEE Trans. Plasma Sci.*, 50(10):3715–3724, Oct. 2022. doi:10.1109/TPS.2022.3203007.

[18] T. Christen and N. Ranjan. "Generalized Mayr Model for Arcs in MV Switches With Splitter Plates". *IEEE Trans. on Power Del.*, 37(1):359–364, Feb 2022. doi:10.1109/TPWRD.2021.3060145.

[19] M. Becerra, J. Nilsson, S. Franke, et al. "Spectral and electric diagnostics of low-current arc plasmas in CO2 with N2 and H2O admixtures". *J. Phys. D: Appl. Phys.*, 57(1), 2024. doi:10.1088/1361-6463/ACFCC6.

[20] T. Billoux, V. Boretskij, Y. Cressault, et al. "Emission spectrum of the electric arc discharge in CO2 between copper electrodes". In *21st Int. Symp. Plasma Chemistry (ISPC 21)*, Cairns, AUS, 2013.

[21] Y. Yokomizu, R. Ochiai, and T. Matsumura. "Electrical and thermal conductivities of high-temperature CO2-CF3I mixture and transient conductance of residual arc during its extinction process". *J. Phys. D: Appl. Phys.*, 42(21), 2009. doi:10.1088/0022-3727/42/21/215204.

[22] L. Zhong, J. Wang, J. Xu, et al. "Effects of Buffer Gases on Plasma Properties and Arc Decaying Characteristics of C4F7N–N2 and C4F7N–CO2 Arc Plasmas". *Plasma Chemistry Plasma Process.*, 39(6):1379–1396, 2019. doi:10.1007/S11090-019-10015-8.

[23] M. Seeger. "Environmentally friendly high-voltage AC switching technology: gas circuit breakers with SF6 alternative gases". In K. Niayesh, editor, *Green HV Switching Technologies for Modern Power Networks*, pages 227–312. IET, London, UK, 2023. doi:10.1049/PBPO236E_ch4.